Paleoproductivity proxies and alkenone precursors in the Western Mediterranean during the Early-Middle Pleistocene transition

Maria Marino [a], Teresa Rodrigues [b c], Ornella Quivelli [a], Angela Girone [a],

Patrizia Maiorano [a], Franck Bassinot [d]

[a]Dipartimento di Scienze della Terra e Geoambientali, Università degli Studi di Bari Aldo Moro, Via E. Orabona 4, 70125 Bari, Italy

[b]Divisão de Geologia e Georecursos Marinhos, Instituto Português Do Mar e da Atmosfera, Rua Alfredo Magalhães Ramalho, 6, 1495-006 Lisboa, Portugal

[c]Centro de Ciências Do Mar (CCMAR), Universidade Do Algarve, Campus de Gambelas, 8005-139 Faro, Portugal

[d]Laboratoire des Sciences Du Climat et de L'Environnement, Domaine Du CNRS, Gif-sur-Yvette 91198, France

Highlights

Coccolithophores, $\delta^{18}O$, SST, C_{37}-alkenones were studied at Site 975 (MIS 20-MIS 19).

Coccolithophore paleoproductivity (NAR and C_{37}) proxies were compared to API and SST.

Unsaturated C_{37} compounds were compared to alkenone-producing species.

Diverse gephyrocapsids (species and morphotypes) produced alkenones through time.

SST, nutrient and oceanography controlled species abundance and alkenone concentration.

Abstract

Multidisciplinary analyses (taxonomic analysis of coccolithophore assemblages, stable oxygen isotopes, marine and terrestrial biomarkers) have been carried out on sediments from Ocean Drilling Program Site 975 in the Algero-Balearic basin, through late marine isotope stage (MIS) 20-19 (800–756 ka). The aim is to compare coccolithophore paleoproductivity proxies, such as C_{37} alkenone concentration and nannofossil accumulation rate (NAR), and understand their relationship with paleoceanographic condition and paleoenvironmental changes, alkenone-producing precursors and unsaturated C_{37} alkenone compounds. The patterns of C_{37} alkenones and NAR provide reliable information on past paleoproductivity changes since coccolith dissolution and organic matter preservation were excluded as relevant processes at the site. This is testified by the high values of Nannofossil Dissolution Index and relation between C_{37} alkenone concentration and Alcohol Preservation Index, the latter used as a proxy of sea bottom ventilation in the basin. A weak mismatching between NAR and C_{37} alkenone concentration

records has been observed and related to paleoenvironmental factors and ecological preferences of alkenone-producing species. Temperature variations mostly controlled the alternating interspecific abundance variations of these taxa through glacial-interglacial and stadial-interstadial climate phases. The percentage abundances of alkenone-producing species, *Gephyrocapsa caribbeanica* and *Gephyrocapsa* with open central area (mainly *G. margerelii-G. muellerae*) strongly co-varied with the percentages of $C_{37:2}$ and $C_{37:3}$, respectively during warm and cool-cold periods, suggesting their prominent role in producing these unsaturated C_{37} alkenone compounds. Moreover, *Gephyrocapsa* spp. with open central area > 3 µm were likely the main $C_{37:4}$ producers during the colder late MIS 20 stadial and stadial phases. Other factors in addition to temperature influenced the paleoproductivity proxy patterns. The oceanographic condition established during MIS 20-MIS 19 deglaciation and the more nutrient-rich surface waters during the orbitally-controlled organic-rich layer deposition in the early MIS 19 enhanced primary productivity leading to higher production and preservation of total C_{37} alkenones.

Keywords

Coccolithophores, Marine and terrestrial biomarkers, δ18OG. Bulloides, Alkenone-SST, Algero-Balearic basin, MIS 20-MIS 19

1. Introduction

Alkenones are molecular biomarkers synthesized by a small group of haptophyte algae, which in the modern ocean is mainly represented by two coccolithophore species of the Noelaerhabdaceae family, *Emiliania huxleyi* and *Gephyrocapsa oceanica* (Marlowe et al., 1990; Volkman et al., 1980a, Volkman et al., 1980b, Volkman et al., 1995). The first occurrence of alkenones is from Cretaceous sedimentary records and was attributed to calcareous nannoplankton producers based on the phylogenetic affinities of alkenones in extant species (Farrimond et al., 1986; Brassell et al., 2004). Several members from the Noelaerhabdaceae, such as *Dictyococcites* spp., *Cyclicargolithus* spp., *Reticulofenestra* spp. and *Pseudoemiliania lacunosa*, are considered the most probable alkenone producers in sediments deposited since the Eocene (Marlowe et al., 1990; Beltran et al., 2007, Beltran et al., 2011; Henderiks and Pagani, 2007; Bolton et al., 2010; Plancq et al., 2012; Athanasiou et al., 2017). *Gephyrocapsa caribbeanica* has been also regarded as a potential alkenone producer during Pleistocene in the North Atlantic (Palumbo et al., 2013) and Indian (Tangunan et al., 2021) oceans, and in

Mediterranean Sea during MIS 20-MIS 19 (Maiorano et al., 2021). In addition, alkenone production has been reported for some species of the non-calcifying haptophyte genera Chrysotila and Isochrysis, the latter considered as an ingroup of the *Emiliania–Gephyrocapsa* clade (Fujiwara et al., 2001). These noncalcifying genera are characteristic of coastal/brackish waters (Conte et al., 1994; Marlowe et al., 1984, Marlowe et al., 1990; Versteegh et al., 2001; Volkman et al., 1989; Rontani et al., 2004), although Isochrysis strains have been observed in open ocean sediments (Versteegh et al., 2001).

Although a number of papers is available on the past alkenone producers (e.g. Sicre et al., 2000; Villanueva et al., 2002; Beltran et al., 2011; Rosell-Melé et al., 2011; Plancq et al., 2012; Athanasiou et al., 2017), additional data are necessary to better quantify their past paleoproductivity and their connection with environmental parameters and alkenone concentration (Volkman, 2000). The main proxies used to reconstruct coccolithophore paleoproductivity are total C37 alkenone concentration and nannofossil absolute abundance and/or nannofossil accumulation rate – NAR (Sicre et al., 2000; Villanueva et al., 2001; Baumann et al., 2004; Emanuele et al., 2015; Athanasiou et al., 2017; Quivelli et al., 2020; Raja and Rosell-Melé, 2021). Under good preservation conditions (i.e. insignificant coccolithophore dissolution and alkenone degradation), and reduced contribution from non-calcifying species or limited dilution effects (Beltran et al., 2011; Plancq et al., 2014; Plancq, 2015; Prahl et al., 1989; Malinverno et al., 2008; Maiorano et al., 2021), the alkenone concentration in sediments should reflect the number of coccoliths of alkenone-producing taxa (Plancq et al., 2014). Such approach has been used to identify alkenone-producing species in sediments from the Oligocene-Miocene (Plancq et al., 2012), Pliocene (e.g., Bolton et al., 2010; Beltran et al., 2011; Athanasiou et al., 2017), and late Quaternary (e.g., Müller et al., 1997; Weaver et al., 1999; Sicre et al., 2000; Herbert, 2001; Rodrigues et al., 2011, Rodrigues et al., 2017; Palumbo et al., 2013).

The relation between coccolithophore species precursors and C37 alkenones with different degree of unsaturation (C37:2, C37:3, C37:4) are still poorly known in the fossil records, yet some robust pieces of information can be obtained on paleo-environmental conditions. It has been suggested that the tetra-unsaturated alkenone (C37:4) can be used as an indicator of paleo-salinity changes, since alkenone producers tend to produce more C37:4 in cold and low salinity environment (Rosell-Melé, 1998). This biomarker has been successfully applied to study salinity variations in oceanic regions (Bard et al., 2000; Harada et al., 2003; Rosell-Melé,

1998; Sicre et al., 2002; Seki et al., 2005; Martrat et al., 2007; Rodrigues et al., 2017) and capture signal of melting water influx into the Mediterranean Sea (e.g. Martrat et al., 2004; Quivelli et al., 2021). West of the Iberian Margin, during the Younger Dryas, high percentages of unsaturated C37:4 alkenones are coeval with peaks of Gephyrocapsa muellerae relative abundances, a signal of cold fresh water masses recorded in sediments from the Tagus pro-delta site D13882 (Rodrigues et al., 2010). Recently, the C37:4 concentrations have been associated with the alkenone producer Isochrysidales "Group 2i" (e.g., Isochrysis galbana, Ruttnera lamellosa) and positively correlated with annual mean sea ice concentrations, thus suggesting that high %C37:4 is a proxy of sea ice rather than salinity (Wang et al., 2021, cum references therein).

The di-unsaturated and tri-unsaturated C37 alkenones (C37:2 and C37:3, respectively) are ubiquitous and abundant in marine sediments, and their production is linked to the coccolithophore growth temperature (e.g. Brassell et al., 1986; Prahl and Wakeham, 1987; Herbert, 2014). In particular, in cold conditions, coccolithophore species generate higher relative amounts of the more unsaturated forms (C37:3 and C37:4), while in warmer waters the di-unsaturated compound (C37:2) prevails, as demonstrated through culture experiments of E. huxleyi (Brassell et al., 1986; Kitamura et al., 2018; Prahl et al., 2000).

Although some studies have indicated that alkenones may be susceptible to degradation (e.g. Conte et al., 1992; Rontani et al., 2009, Rontani et al., 2013; Ausín et al., 2021), the ratio of unsaturation degree in the sediment is considered a useful tool for sea surface paleotemperature estimates through the Uk'37 unsaturation index (Volkman et al., 1980a, Volkman et al., 1980b; Prahl et al., 1989; Madureira et al., 1995; Sicre et al., 1999). The Uk'37, calibrated based on coccolithophore cultures of E. huxleyi and G. oceanica and modern core top sediments (e.g., Prahl et al., 1988; Conte et al., 1995, Conte et al., 2006; Müller et al., 1998; Riebesell et al., 2000), seems to be species-dependent (e.g., Volkman et al., 1995; Conte et al., 1998) and even species strain-dependent (e.g. E. huxleyi var. aurorae and var. huxleyi, Rigual-Hernández et al., 2022). This index and its relationship with temperature seem to be valid prior to the Quaternary when different precursors produced alkenones (e.g. mainly reticulofenestrids during the Eocene-Oligocene, Plancq et al., 2014), suggesting that ancient alkenone producers were phyletically related to modern producers. Besides, no rich assessments on the strict relation between the specific C37 alkenone unsaturated compounds

and the coccolithophore precursors are available for Pleistocene interval with dominant gephyrocapsid species. Because paleoecology of the mid-Pleistocene gephyrocapsids is rather well known, this may further advantage the interpretation of their relationship with C37 alkenone concentration and relative proportions of unsaturated alkenone compounds.

Here we propose the study of two coccolithophore paleoproductivity proxies (C37 alkenone concentration and NAR) during the mid-Pleistocene, combined with the changes in alkenone unsaturated compounds (C37:2, C37:3, and C37:4) and relative abundance of coccolithophore species through time. This in order to improve knowledge on relationship between paleoproductivity proxies and past environmental and ecological factors and on the potential mid-Pleistocene coccolithophore precursors. For this purpose, we present high-resolution quantitative data (down to 200 year-resolution) of i) total C37 alkenone concentration and percentages of alkenone unsaturated compounds, ii) quantitative abundances of potential species precursors, iii) absolute coccolith abundance and nannofossil accumulation rate, and iv) alkenone-SST. The multiproxy paleoenvironmental framework is integrated in the detailed chronostratigraphic and climatic framework provided by the high-resolution δ18OG.bulloides record over the interval 800–756 ka. Nannofossil dissolution index (DI) and alcohol preservation index (API) have been also estimated in order to better evaluate the preservation of coccoliths and deep-sea ventilation, respectively. The study was performed on samples from the Ocean Drilling Program (ODP) Site 975, in the Algero-Balearic basin, through late marine isotope stage (MIS) 20 – MIS 19, a crucial time of the mid-Pleistocene transition characterized by multiple climate oscillations and thus particularly suitable to detect paleoenvironmental changes and switches between potential precursors with different ecological preference. Moreover, MIS 19 is an interesting key mid-Pleistocene marine isotope stage since, from an orbital point of view, is comparable to the current interglacial (Holocene) by sharing a quasi-similar precession and low eccentricity parameters (Tzedakis et al., 2012), that controlled the primary productivity in the oceans (i.e. Rickaby et al., 2007; Beaufort et al., 2021). The Algero-Balearic Sea is one of the most productive areas of the Mediterranean basin, with an “intermitted” productivity pattern (D'Ortenzio and Ribera d'Alcalà, 2009), and has varied due to changes in the water column structure and western Mediterranean deep-water strength at glacial-interglacial and millennial scales (Rohling et al., 2015, cum references therein).

2. Material

Ocean Drilling Program Leg 161 Site 975 was drilled at 2415 m of water depth in a sub-basin on the Menorca continental rise (Fig. 1), between the Balearic Promontory (Menorca and Mallorca Islands) and the South Balearic-Algerian Basin (38°53.8'N, 4°30.6'E) (Shipboard Scientific Party, 1996). Pleistocene sediments through the studied interval mainly consist of calcareous nannofossil clay and calcareous silty-clay with nannofossil dominating over foraminifer component (Shipboard Scientific Party, 1996).

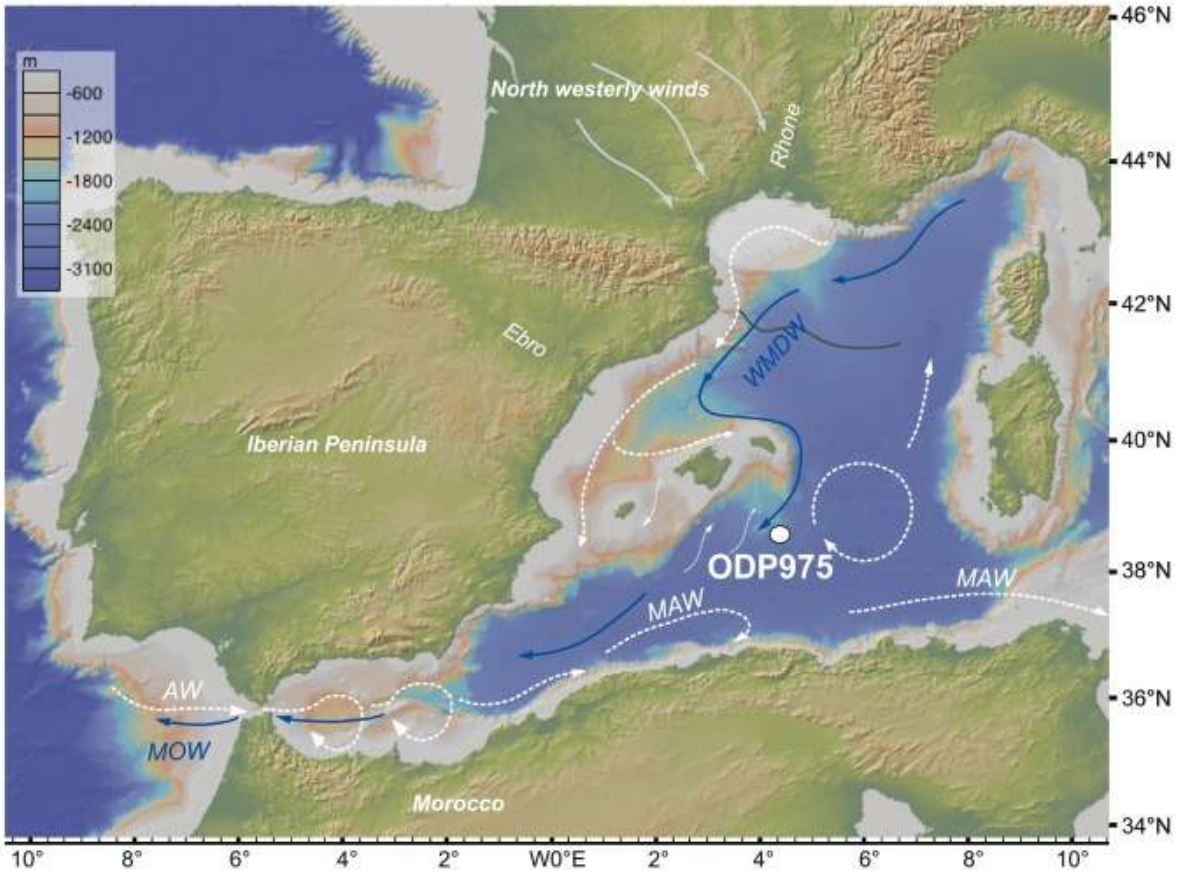

Fig. 1. Location map of ODP Site 975. White dashed arrows are the main sea surface currents: AW: Atlantic waters, MAW: modified Atlantic waters. Blue arrows indicate deep waters: WMDW: western Mediterranean deep waters, which forms in the Gulf of Lion (dashed area); MOW: Mediterranean outflow waters. Northwesterly winds are drawn as light blue arrows. Modified from Millot (1999) and Frigola et al. (2008).

One hundred forty-three samples were analyzed from Hole C (cores 7–8), between 66.53 and 62.97 mcd (meter composite depth) for oxygen isotopes, molecular biomarkers and coccolithophores. Sedimentation rate varied between about 5 and 10 cm/ky through MIS 20-

18, according to the age model of Pierre et al. (1999), which relies on the calibration of the δ18O record of the planktonic foraminifer Globigerina bulloides to the orbital time scales of Shackleton et al. (1990), Bassinot et al. (1994), and Tiedemann et al. (1994). The highest temporal resolution in our record is of about 200 years (a sample every 2 cm), from the interval between 66.35 mcd and 64.53 mcd (from 800.6 ka to 782.1 ka). The intervals from 66.53 to 66.37 mcd (802.7 ka to 800.8 ka) and from 64.5 to 62.97 mcd (781.6 ka to 756.5 ka), have been studied at a temporal resolution of about 400 years (a sample every 4 and 3 cm, respectively).

3. Oceanographic setting

The modern Western Mediterranean Sea dynamic is driven by frontal and turbulent regimes, with eddies playing a significant role in the exchange of water masses (Millot, 1999) (Fig. 1). Through the Balearic Channels the meridional exchanges occur between the cooler, more saline waters of the northern basins (Gulf of Lion), and the warmer, fresher waters of the southern basins (Alboran and Algero–Balearic basins) (Pinot et al., 2002). Surface waters are composed of low-salinity and cold, nutrient-rich Atlantic waters, which are progressively modified by air–sea interactions, which turns them into warmer and saltier Modified Atlantic Water (MAW) (Fig. 1). The MAWs flow eastward along the Algerian slope and form the Algerian Current that branches off northerly and forms several large-scale cyclonic gyres reaching the Balearic Islands (Millot, 1999). A permanent cyclonic gyre develops in the Gulf of Lion where the Northern Balearic Front separates the older, cold and more saline surface waters flown along the northern European coasts, towards the west, from the eddies deriving from the warmer and less saline MAW (Millot, 1999). The Mediterranean Intermediate Water (MIW), also known as Levantine Intermediate Water (LIW), flows westward below the MAW (Cramp and O'Sullivan, 1999). The MIW originates in the eastern Mediterranean basin as a result of evaporation and increasing salinity in summer, and relatively deep vertical mixing triggered by intense dry northerly winds in winter (Bryden and Stommel, 1982; Lascaratos et al., 1999). The Western Mediterranean Deep Water (WMDW) is the deepest water mass forming via deep convection in the Gulf of Lion (Fig. 1) (Benzohra and Millot, 1995). The WMDW production is controlled by wind strength, initial density of source waters, and the circulation patterns (Pinardi and Masetti, 2000). The major force driving deep water formation is represented by north-westerlies, which enhance thermohaline circulation (Millot, 1990, Millot, 1999; Leaman and Schott, 1991). Dense Shelf Water Cascading (DSWC) is currently recorded during extreme

cold and windy winters, when large volumes of dense water are formed on the continental shelf of the Gulf of Lion, transporting large quantities of organic matter and sediments to deeper depths (Canals et al., 2006). These deep waters supply oxygen to the deeper layers in the Mediterranean Sea, as well as debris inputs (Pinardi et al., 2006; Jimenez-Espejo et al., 2007, Jimenez-Espejo et al., 2008), that mainly come from the Ebro and Rhone fluvial discharges (Martin et al., 1989). The Algero-Balearic Basin is considered one of the most productivity Mediterranean areas, with intermittently primary productivity blooming (D'Ortenzio and Ribera d'Alcalà, 2009).

4. Methods

4.1. Oxygen isotopes and age model

Four to fifteen specimens of *Globigerina bulloides* (250–315 μm) were picked for measurement of stable oxygen and carbon isotope analysis. All analyses were performed on an Isoprime 100 (Elementar) dual-inlet Isotope Ratio Mass Spectrometer (Elementar) at the Laboratoire des Sciences du Climat et de l'Environnement (LSCE). The results are expressed as $\delta^{18}O$ vs V-PDB (in ‰) through calibration to international NBS standards. The external analytical reproducibility determined from replicate measurements of a carbonate standard is ±0.05 ‰ (1σ). We used the age model of Pierre et al. (1999), which rests upon the tuning of the *Globigerina bulloides* $\delta^{18}O$ record to orbitally-derived age models of planktonic records from Shackleton et al. (1990), Bassinot et al. (1994), and Tiedemann et al. (1994). We constructed the age-depth profile by linear interpolation between tie-points of Pierre et al. (1999).

4.2. Marine biomarkers and alkenones SST, and API

The total C_{37} alkenone concentrations have been obtained according to the analytical procedure described in detail elsewhere (see Villanueva and Grimalt, 1997; Rodrigues et al., 2009, Rodrigues et al., 2017; Quivelli et al., 2020, Quivelli et al., 2021). It has been used as paleoproductivity indicator (Schubert et al., 1998; Schulte et al., 1999; Villanueva et al., 2001) and useful to estimate past phytoplankton biomass in different oceanographic settings (Raja and Rosell-Melé, 2021). The percentages of di-, tri-, and tetra-unsaturated alkenones have been discriminated to compare their distribution with the percentage abundance of potential species precursors. Sea surface temperature (SST) has been estimated calculating the

alkenone $U^{k'}_{37}$ index that is based on the di- and tri-unsaturated alkenone ratio [($C_{37:2}$)/($C_{37:2}$ + $C_{37:3}$)] (Prahl and Wakeham, 1987) and converted into temperature values using the global core top calibration of annual SST [$U^{k'}_{37}$ = (0.033*SST) + 0.044] (Müller et al., 1998), with a methodology uncertainty of ±0.5 °C. Tetra-unsaturated compound ($C_{37:4}$) has been considered as an indicator of lower temperature and low salinity waters (e.g. McClymont et al., 2008; Rodrigues et al., 2010) and possibly linked to polar and subpolar water influx into the Western Mediterranean (Martrat et al., 2004; Quivelli et al., 2021). Higher plant biomarkers, such as odd carbon numbered ($C_{23–C31}$) *n*-alkanes and *n*-alkanols with even carbon numbered ($C_{22–C30}$), have been quantified to provide the API. The API is obtained by the relative proportion of *n*-hexacosan-1-ol (C_{26}OH) to the sum of C_{26}OH plus *n*-nonacosane (C_{29}) [API = C_{26}OH/(C_{26}OH + C_{29})]. API has been used as a proxy of seafloor oxygenation and organic matter preservation (Poynter and Eglinton, 1991; Cacho et al., 2000; Martrat et al., 2007) in relation to the strength of deep water circulation (western Mediterranean deep waters – WMDW) in the Algero-Balearic Sea (Quivelli et al., 2021), having both *n*-alkan-1-ols and *n*-alkanes the same source and being *n*-alkan-1-ol more prone to degradation with respect to *n*-alkanes that are more resistant (Poynter and Eglinton, 1991; Westerhausen et al., 1993; Bogus et al., 2012; Cacho et al., 2000; Martrat et al., 2007; Quivelli et al., 2020). In this study, high values of API indicate low sea bottom ventilation and slow-shutdown of WMDW.

4.3. Coccolithophore assemblages

Slides for coccolithophore analysis were prepared according to the method of Flores and Sierro (1997) to estimate absolute coccolith abundances. Quantitative analyses were performed using a polarized light microscope at 1000 × magnification and abundances were determined by counting at least 500 coccoliths of all sizes, in a varying number of fields of view, mainly from 5 to 15, rarely up to 30. Total abundances of coccoliths are expressed as N (coccoliths x g^{-1}) and Nannofossil Accumulation Rate (NAR) (coccoliths x cm^{-2} x kyr^{-1}) according to Flores and Sierro (1997): NAR = N x w x S, where N is coccolith/g, w is the wet bulk density (g x cm^{-3}) provided by Comas et al. (1996), S is sedimentation rate (cm x ky^{-1}). NAR is here considered a proxy of paleoproductivity (Steinmetz, 1994; Baumann et al., 2004). Abundances of taxa are expressed as percentage and NAR. Nannofossil dissolution index (DI) has been calculated according to Dittert et al. (1999) modified by Amore et al. (2012): small gephyrocapsids/(small gephyrocapsids + *Calcidiscus leptoporus*). The taxonomy of gephyrocapsids, which are a major

component of the assemblage, follows the criteria adopted in Maiorano et al. (2013, and references therein) based on the size, width of central area and/or angle bridge to long axis of placolith. Specifically: *Gephyrocapsa* < 3 µm (*G. caribbeanica* with closed central area and gephyrocapsids with open central area); *G. caribbeanica* > 3 µm with closed central area; *G. oceanica* (3.5–5.5 µm) has open central area and angle bridge >50°; *G. margerelii/G. muellerae* (3–4 µm) is a group of gephyrocapsids having open central area and angle bridge between 25° and 40°.

5. Results

5.1. Oxygen isotopes curve

Globigerina bulloides $\delta^{18}O$ record varies between 1.01 and 3.26 ‰ throughout the studied interval (Fig. 2A). After recording heavier values during glacial MIS 20, $\delta^{18}O_{G.bulloides}$ curve slowly depict the MIS 19c displaying decreasing values from 2.5 to 1‰ with low amplitude fluctuations. From 773.6 ka to 756 ka, superimposed on the general trend of increasing values, secondary oscillations are recorded (± 1‰). A first interval with heavier $\delta^{18}O$ values up to 2‰ is recorded near 772.6 ka marking MIS 19b, followed by three distinct increasing peaks centered at about 767.7 ka (−0.08 ‰), 761.8 ka (−0.21 ‰), and at 757.9 ka (−0.44 ‰) (Fig. 2A), which outline stadial phases in MIS 19a. They are interspersed by three marked $\delta^{18}O$ depletion intervals (772.2 ka–768.2 ka, 765.8 ka–762.8 ka, and 760.8 ka–758.9 ka), which are interstadial phases before the MIS 18 glacial inception (Fig. 2A). Following the nomenclature used by Nomade et al. (2019) in MIS 19a, the three interstadial oscillations have been named MIS 19a-1, 19a-2, 19a-3.

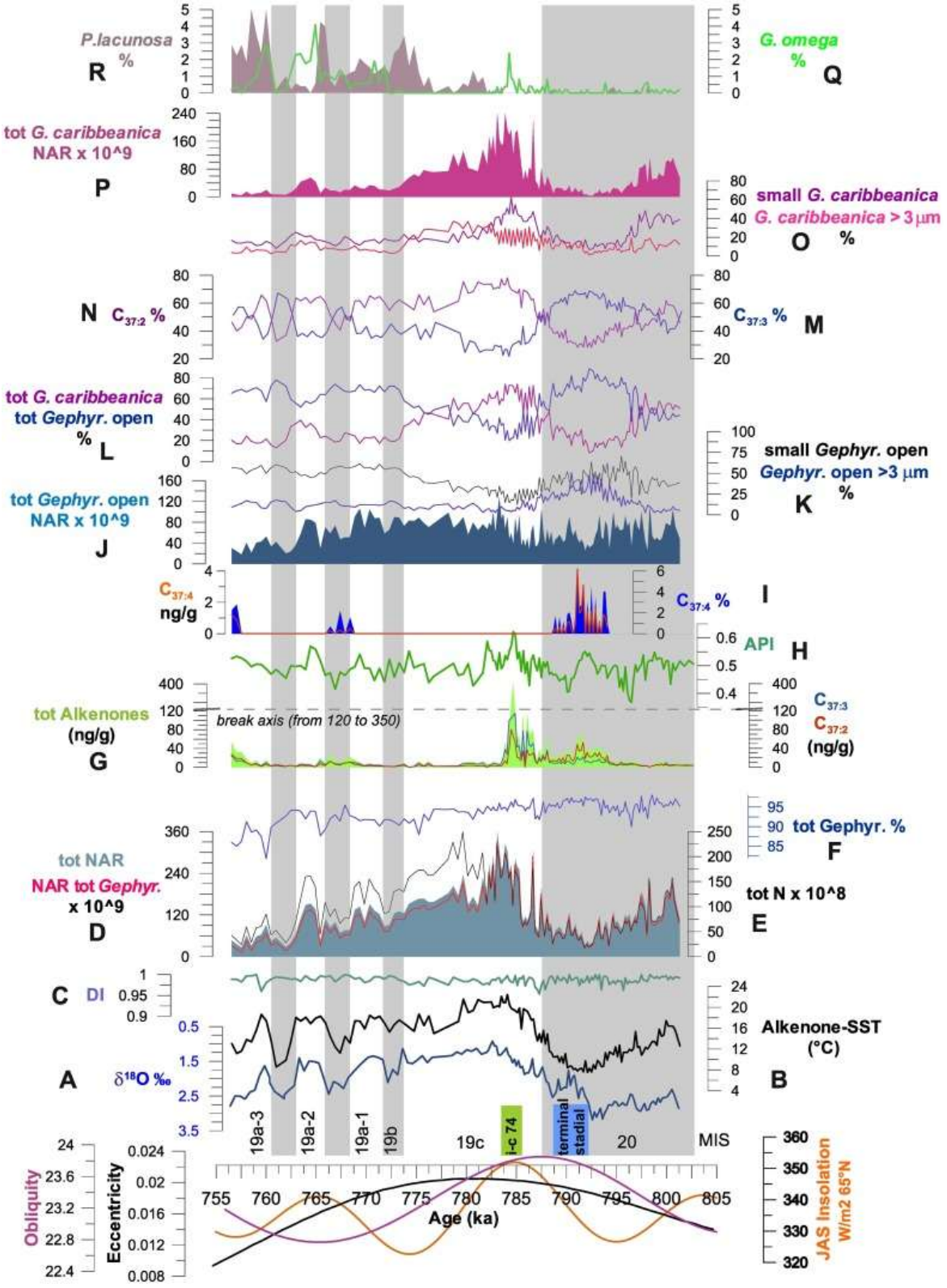

Fig. 2. Comparison between $\delta^{18}O_{G.bulloides}$ (A) at Site 975 and other paleoenvironmental and paleoproductivity proxies. B: alkenone-SST, C: nannofossil dissolution index (DI) according to Dittert et al. (1999) modified by Amore et al. (2012); D: total Nannofossil Accumulation Rate (NAR) and NAR of total gephyrocapsids (coccoliths x cm^{-2} x kyr^{-1}); E: N (coccoliths x g^{-1}); F: percentage abundances of total gephyrocapsids; G: total C_{37} alkenones (ng/g) with $C_{37:2}$ and $C_{37:3}$ (red and blue, respectively); H: alcohol

preservation index (API); I: percentage and ng/g of $C_{37:4}$; J: NAR of total *Gephyrocapsa* open central area (mainly *G. margerelii-G. muellerae*) (coccoliths x cm^{-2} x kyr^{-1}); K: percentages of *Gephyrocapsa* with open central area with morphotypes > and < 3 μm (blue and black lines, respectively); L: percentages of total *G. caribbeanica* and *Gephyrocapsa* with open central area marked as violet and blue lines, respectively; M: percentage of $C_{37:3}$; N: percentage of $C_{37:2}$; O: percentages of *G. caribbeanica* > and < 3 μm (violet and blue lines, respectively); P: NAR of total *G. caribbeanica* (coccoliths x cm^{-2} x kyr^{-1}); Q: percentage of *P. lacunosa*; R; percentage of *G. omega*. Interstadials in MIS 19a are named according to Nomade et al. (2019). Terminal stadial in late MIS 20 is drawn according to Quivelli et al. (2021), ORL i-cycle 74 is traced according to Quivelli et al. (2020). On the left eccentricity, obliquity and mean summer insolation 65°N (W m^{-2}) by Laskar et al. (2004).

5.2. C_{37} alkenones, SST and alcohol preservation index

The total C_{37} alkenone concentration mainly varies from values close to 10 ng/g to values of 400 ng/g (Fig. 2G). The long trend shows a clear increase in the concentration during deglaciation from about 795 to 785.5 ka, followed by the highest values at 784.7 ka. The concentrations sharply decrease after this event and maintain low values during the entire interglacial period until to about 758 ka, where a progressive increase is observed may be marking the inception of MIS 18.

Alkenone-SST record (Fig. 2B) displays glacial-interglacial and stadial-interstadial oscillations with a pattern similar to the $\delta^{18}O_{G.bulloides}$ profile, with higher temperature during low $\delta^{18}O$. The lowest temperatures (< 12°C) were recorded in the late MIS 20, partially concurrent with relative lightening of $\delta^{18}O$. While, the lowest portion of the studied MIS 20 was warmer than 12°C. During MIS 19c, with the exception of an abrupt decrease of about 4°C at 785.5 ka, in the mid of ORL, temperatures were warmer than 15°C, recording higher values between 19 and 22°C from 784.3 ka to 779.2 ka. Looking at the SST record, temperatures were not so cold as expected during MIS 19b reaching 15.2°C, whereas they display a general decreasing trend since 780 ka upwards, marked by three abrupt significant coolings centered at 767.4 ka (11.2°C), at 761 ka (8.5°C), and at 757.1 ka (11°C), alternating with three respective warming phases during MIS 19a-1 (up to 18.4°C at 779.3 ka), MIS 19a-2 (up to 18.2°C) and MIS 19a-3 (up to 18.6°C).

While the absolute abundances of $C_{37:3}$ and $C_{37:2}$ have the same pattern ($r = 0.86$, $p < 0.0001$, $n = 136$) (Fig. 2G), the percentages of $C_{37:3}$ and $C_{37:2}$, which represent the main component (up to 94%) of the total alkenones, as expected show an evident opposite pattern ($r = -0.8$, $p < 0.0001$, $n = 136$), being % $C_{37:3}$ more abundant mainly during glacial and stadial phases and the $C_{37:2}$ dominant during interglacial and interstadial phases (Fig. 2 M and

N). The higher percentage of $C_{37:4}$ has been detected during late MIS 20, between 794 ka and 788.5 ka (Fig. 2I), displaying fluctuating values up to ~6% at 791.1 ka, interpreted as signal of cold low salinity melting waters at the site location during the terminal stadial of MIS 20 (Quivelli et al., 2021). Upwards, $\%C_{37:4}$ is absent with two exceptions recording percentage under 2%, at 768.4–766.4 ka and at 757.1 ka.

The API (Fig. 2H) displays values between 0.36 and 0.62, recording the minimum values during glacial MIS 20 and maximum value during the late MIS 20-lower MIS 19 ORL deposition (Quivelli et al., 2020). From MIS 19c upward, API displays small fluctuations (± 0.10) near the average value of 0.50, increasing during MIS 19a-1, 19a-2 and 19a-3 with values around 0.55–0.57, before MIS 18 inception (Fig. 2H).

5.3. Coccolithophore assemblages

Coccolithophores assemblages are well preserved throughout the whole investigated section since values of DI are always close to 1 (> 0.95) suggesting no important dissolution effects on coccoliths (Fig. 2C). The total N varies from 20×10^8 to 250×10^8 coccoliths x g^{-1} (Fig. 2E, black line). The total NAR ranges between 25×10^9 and 355×10^9 coccoliths/cm^2kyr, with a mean value per sample of 126×10^9 coccoliths/cm^2kyr (Fig. 2D). The patterns of N and NAR show similar trends and higher values are recorded during interglacial MIS 19c and interstadials of MIS 19a.

The assemblage is mainly composed of gephyrocapsids with relative contributions higher than 90% (Fig. 2F red line, J, P). Taxa with lower percentage abundances are represented by *Umbilicosphaera* spp., *Helicosphaera* spp., *Rhabdosphaera* spp., *Calciosolenia* spp., *Oolithotus* spp., *Florisphaera profunda, Syracosphaera* spp., *Calcidiscus* spp., *Pseudoemiliania lacunosa*, *Rhabdosphaera* spp. and *Coccolithus* spp. Subordinate taxa also include *Reticulofenestra* sp. >3 µm, *Pontosphaera* sp., and holococcoliths, with very rare and scattered occurrences.

Results shown in the present paper incorporate some of data published in Quivelli et al., 2020, Quivelli et al., 2021 relative to the interval from 800 ka to 779 ka. Such data (total NAR, NAR and percentages of small gephyrocapsids and total *G. margerelii-G. muellerae*, total C_{37} alkenone concentration, $\%C_{37:4}$, API, $\delta^{18}O_{G.bulloides}$), combined with the new results for the whole investigated interval (800–755 ka), including the direct comparison between the main

representatives coccolithophores species and the different alkenone unsaturated compounds improve paleoproductivity reconstruction and our knowledge to understand the specific precursor of the alkenones throughout late glacial MIS 20-interglacial MIS 19.

6. Discussion

6.1. Paleoproductivity proxies and relation with paleoenvironmental parameters

The coccolithophore assemblages and fluxes benefited from warmer conditions in sea surface waters during interglacial phase MIS 19c and interstadials of MIS 19a as evidenced by the patterns of total N and total NAR records, which show positive correlation with higher alkenone-SST and lighter $\delta^{18}O$ values (Fig. 2B, D and E). This result is coherent with data from the contemporary central Mediterranean on land marine Montalbano Jonico record (Ionian Sea, Marino et al., 2020; Maiorano et al., 2021). Conversely, the total C_{37} alkenone profile does not follow the same oscillations of alkenone-SST ($r = + 0.12$, $p < 0.14$, $n = 136$) nor the pattern of NAR (and N) ($r = + 0.16$, $p < 0.05$, $n = 136$) (Fig. 2 D–F). This could suggest a possible bias associated with carbonate dissolution and/or biomarker degradation. However, our observations do not support the assumption that coccolith dissolution is responsible for the patterns seen in N and NAR records and for the mismatch between C_{37} alkenones and NAR considering the good coccolith preservation (high values of DI, Fig. 2C) throughout the entire investigated interval. Furthermore, the weak relationship between the C_{37} alkenone and the API profiles ($r = + 0.42$, $p < 0.0001$, $n = 136$) (Fig. 3a) through the whole investigated interval suggests that oxidation of alkenones was not a significant process associated with changes in past dynamics of WMDW. Because weak or suppressed WMDW (high values of API) are recorded during low or high total C_{37} alkenone concentration (Fig. 2), we could conclude, although with caution, that changes in the total C_{37} alkenone concentration likely reflect a genuine signal of alkenone production/accumulation over the studied section. Nonetheless, it can be noted that in the lower part of the studied site (from ca. 795 to 782 ka), a positive influence of decreased deep-water circulation on C_{37} alkenone preservation is suggested by the higher values of total C_{37} alkenone concentration that positively correlate to higher API ($r = + 0.6$, $p < 0.0001$, $n = 60$) (Fig. 3b). This late MIS 20-early MIS 19 interval actually corresponds to the deglaciation and the beginning of oceanographic conditions that promoted higher primary productivity and the deposition of the organic-rich layer (ORL) associated with insolation cycle 74 (see discussion in Quivelli et al., 2020, Quivelli et al., 2021), when NAR reaches the higher

values. The peculiar orbitally-controlled (summer insolation maximum, Fig. 2A) hydrologic feature in the Western Mediterranean associated with deglaciation and weaker or even WMDW shut down (high API) may have further favored the preservation of the increased organic matter supply to the sea bottom during higher primary productivity, the latter promoted by the nutricline shallowing and nutrient enrichment in the photic zone (Quivelli et al., 2020). Through this particular oceanographic condition, total C_{37} alkenone concentration shows higher values during both late MIS 20, when alkenone-SST and N and NAR decrease, and during early MIS 19 up to about 782 ka, when temperature, N and NAR increase (Fig. 2). During these periods, in fact, very weak relation seems to occur between alkenone-SST and total C_{37} alkenone concentration ($r = + 0.3$, $p < 0.005$, $n = 60$) and between the latter and total N or NAR ($r = + 0.2$, $p < 0.09$, $n = 60$). Following the end of ORL upwards, the pattern of total NAR does not match that of total C_{37} alkenone ($r = -0.3$, $p < 0.01$, $n = 48$), and the API and total C_{37} alkenone concentrations are not significantly correlated ($r = + 0.16$, $p < 0.24$, $n = 48$) (Fig. 2).

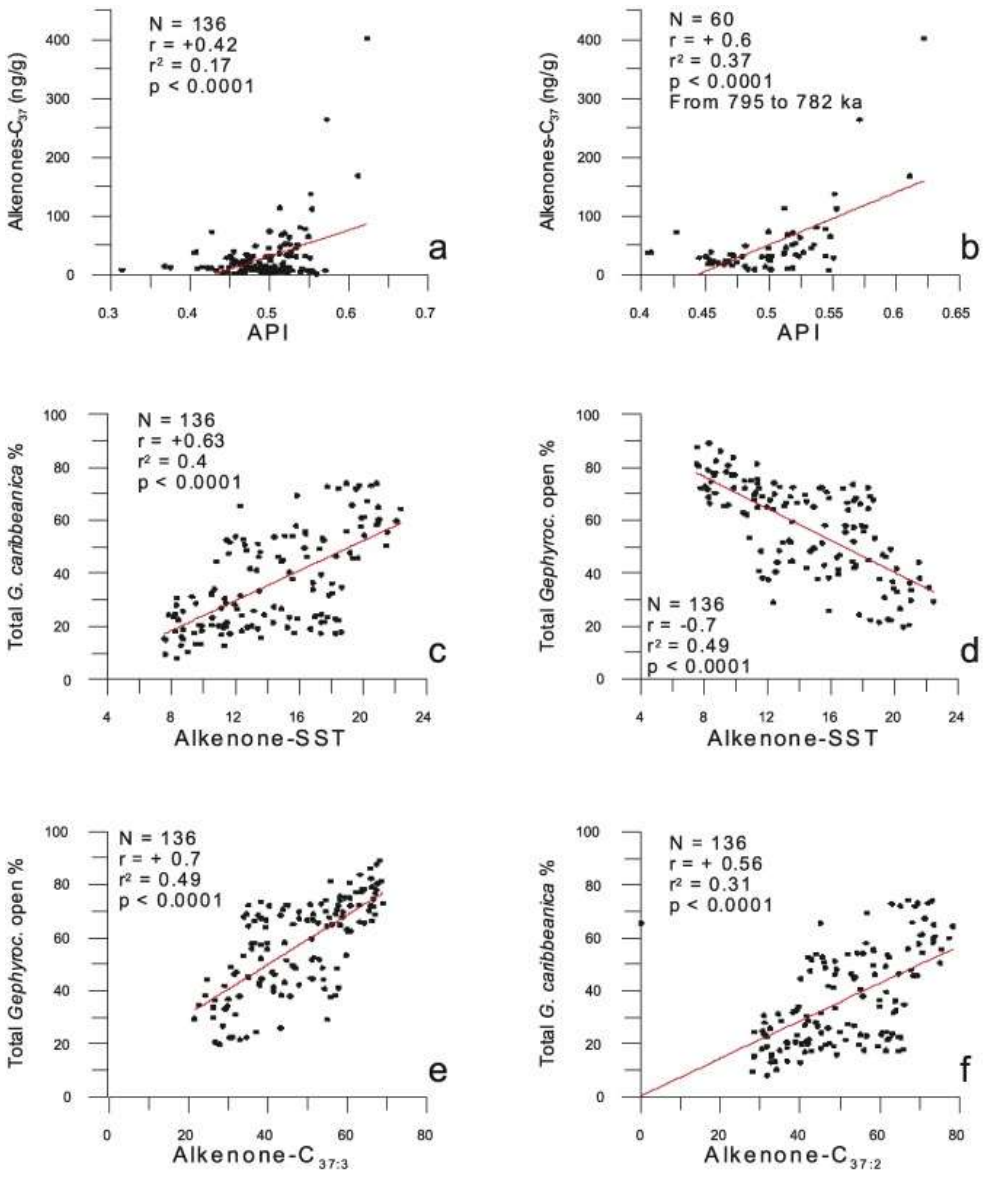

Fig. 3. Scattered plots of different variables at Site 975 based on Pearson correlation results.

Our data on paleoproductivity proxies and environmental parameters allow us to outline the following assumptions: i) excluding the deglaciation and ORL periods (see above), WMDW dynamics did not significantly influence the organic matter preservation, suggesting that total C_{37} alkenone profile could represent a primary signal not affected by sea bottom ventilation, ii) the two coccolithophore paleoproductivity proxies (NAR and total C_{37} alkenones) are not well correlated each other, since high amounts of total C_{37} alkenones (Fig. 2G) are recorded either during high and low total NAR (Fig. 2D), as also recorded in Pliocene sediments from the Mediterranean area (Beltran et al., 2011); thus, both paleoproductivity proxies need to be considered in the interpretation of any paleoclimate record to better understand the relationship between paleoproductivity and environmental parameters, and iii) total

C_{37} alkenone may increase or decrease during both high and low alkenone-SST likely in relation with changing abundance through time of alkenone-producing species, depending on their ecological preference, as discussed in the next section. However, some questions exist concerning the relation between C_{37} alkenone concentration and past/modern alkenone-producing species: (1) the amount of alkenones produced per cells by species is not well known in fossil records (see Sicre et al., 2000) and may depend on cell size and growth rate (e.g. Henderiks and Pagani, 2008; Tangunan et al., 2021), (2) in the past, like in modern coccolithophore assemblages, alkenone cellular production may have varied depending on paleoenvironmental conditions (Epstein et al., 1998, Epstein et al., 2001; Pancost et al., 1999; Yamamoto et al., 2000; Volkman, 2000; Malinverno et al., 2008), such as light and nutrient stress (Prahl et al., 2003) and seasonal changes (e.g. Sikes et al., 1997, Sikes et al., 2005; Harada et al., 2006; Max et al., 2020; Rigual-Hernández et al., 2022).

6.2. Alkenone-producing species vs unsaturated alkenone compounds

The percentages of total *Gephyrocapsa* with open central area (mainly *G. margerelii-G. muellerae*) and total *G. caribbeanica* appear perfectly anti-correlated ($r = -0.98$, $p < 0.0001$, $n = 136$) as it may be expected being the main component of the assemblages, and their fluctuations depict repeated switches through time (Fig. 2L). Specifically, the increases of % *G. caribbeanica* (Fig. 2L, violet line) during warmer phases at the site location indicate a primary ecological preference for higher sea surface temperature, in agreement with several records (e.g. Bollmann et al., 1998; Flores et al., 1999; Amore et al., 2012; Maiorano et al., 2013, Maiorano et al., 2015, Maiorano et al., 2016a, Maiorano et al., 2021; Bordiga et al., 2014; Marino et al., 2014, Marino et al., 2018; Saavedra-Pellitero et al., 2017; Toti et al., 2020). An additional evidence of temperature dependence of *G. caribbeanica* is the similar pattern between their NAR (Fig. 2P) and the covariant profiles of total NAR and alkenone-SST (Fig. 2 B–D). On the contrary, *Gephyrocapsa* with open central area (Fig. 2L, blue line) dominated during cold-cool phases (MIS 20 and stadials of MIS 19), and this agrees with biogeographic distribution and paleoecological evidences from ocean records (Samtleben and Bickert, 1990; Bollmann, 1997; Okada and Wells, 1997; Giraudeau et al., 2010; Saavedra-Pellitero et al., 2010; Amore et al., 2012; Marino et al., 2014; Maiorano et al., 2015) and Mediterranean area (e. g. Weaver and Pujol, 1988; Maiorano et al., 2013; Marino et al., 2018). The primary dependence of these taxa on temperature (Bollmann et al., 2002) is

clearly depicted by the linear correlation index value, which, as expected, is positive between alkenone-SST and total % *G. caribbeanica* (r = + 0.63, $p < 0.0001$, $n = 136$), whereas it is negative between SST and total % *Gephyrocapsa* with open central area ($r = -0.7$, $p < 0.0001$, $n = 136$) (Fig. 3c and d). The good agreement between the climate phases drawn by the patterns of planktonic $\delta^{18}O$ and alkenone-SST (Fig. 2A and B) supports the reliability of temperature record at the studied site based on $U^{k'}_{37}$ unsaturation index and validates *Gephyrocapsa* with open central area and *G. caribbeanica* as useful proxy of cold and warm condition, respectively.

The weak matching between total NAR of gephyrocapsids (Fig. 2D, red line) and total C_{37} alkenone concentrations may be also observed when the latter are compared with the percentages of total *Gephyrocapsa* (Fig. 2F). Therefore, we explored the direct relationship between the percentage abundances of each potential alkenone-producing species-morphotypes (Fig. 2K, L, and O) and the percentage of each unsaturated alkenone compounds (Fig. 2M and N), in order to acquire additional information on which/how species contributed to alkenone production through time.

Total *Gephyrocapsa* with open central area (Fig. 2 L, blue line) show the same pattern of variations than the tri-unsaturated alkenone record (Fig. 2M) with a clear positive linear correlation (r = + 0.7, $p < 0.0001$, $n = 136$) (Fig. 3e) suggesting that this taxon could have been the main producer of $C_{37:3}$ during the cold/cool phases. On the opposite, the dominance of total *G. caribbeanica* during warm phases, associated with increasing percentages of di-unsaturated alkenones (Fig. 2N) seems to indicate that this taxon was the main producer of the $C_{37:2}$ (r = + 0.56, $p < 0.0001$, $n = 136$) (Fig. 3f). Such a relationship between taxa and di- and tri-unsaturated alkenones is especially evident in the lower part of the studied record up to MIS 19c (Fig. 2), and reveals, although does not definitively prove, the prevailing and alternating contribution by those species to C_{37} alkenone production, consistently with their primary ecological preference for the changing temperature and the known influence of this parameter on the biosynthesis of undersaturated C_{37} compounds. In line with this reasoning, the higher abundance of *Gephyrocapsa* with open central area > 3 µm in size (Fig. 2K, blue line) in the coldest phase of late MIS 20 (Quivelli et al., 2021) is also associated with the occurrence of tetra-unsaturated alkenone ($C_{37:4}$) (Fig. 2I), pointing out to the potential prominent role of the taxon to produce this unsaturated alkenone compound. The higher abundance of $\%C_{37:4}$ in late

MIS 20, including the terminal stadial, has been associated with the influx of cold low salinity melting waters into the Algero-Balearic Sea, mostly from North Atlantic and/or the hinterland mountain glaciers (Quivelli et al., 2021). Cold and less saline waters would have promoted the proliferation of *G. margerelii-G. muellerae* > 3 μm and the $\%C_{37:4}$ production, concurrent with a prominent peak of the polar-subpolar *Neogloboquadrina pachyderma* (Quivelli et al., 2021), a taxon used as a proxy of southward subpolar shift in the North Atlantic Ocean and meltwater influx into Mediterranean through the Gibraltar Strait (Sierro et al., 2005; Girone et al., 2013; Capotondi et al., 2016; Marino et al., 2018, Marino et al., 2020; Maiorano et al., 2021; Quivelli et al., 2021). Evidence of increased size of gephyrocapsids (Kulhanek et al., 2008; Kulhanek, 2009; Marino et al., 2014; Maiorano et al., 2015) and *Emiliania huxleyi* (Colmenero-Hidalgo et al., 2004; Balestra et al., 2015) during very cold phases has been previously reported, and has been associated with terminal stadials, mid-Pleistocene Heinrich-type events or Heinrich stadial HS1 in Mediterranean Sea (Girone et al., 2013; Maiorano et al., 2015, Maiorano et al., 2016b; Marino et al., 2018; Bazzicalupo et al., 2018; Trotta et al., 2019). In contrast, *Gephyrocapsa* with open central area < 3 μm increased starting from late MIS 19c upwards at the studied site, with percentage even higher than 50%, thus representing almost the major component of total small *Gephyrocapsa* (Fig. 2K, black line). In the same interval small *G. caribbeanica* attest their lower abundance close to about 20% (Fig. 2O, violet line). This anti-covariant pattern between small *G. caribbeanica* and small *Gephyrocapsa* with open central area was likely associated with combined environmental factors in addition to temperature, and maybe with a change in the orbital configuration. Specifically, weaker insolation and obliquity decrease during the MIS 19 eccentricity minimum (lower than 0.02 Wm^{-2}during MIS 19b-a, Fig. 2), resulted in lower seasonal contrast and higher year-round light availability, which accompanying the cooling trend towards the end of MIS 19c enhanced surface water mixing and unstable condition favoring the r-selection behavior of small gephyrocapsids with open central area. Such interpretation agrees with data from the Alboran Sea where coccolithophore assemblages from MIS 20-MIS 19 record (Toti et al., 2020) and the last 25 kyr (Barcena et al., 2004; Ausín et al., 2015a, Ausín et al., 2015b) evidenced the proliferation of small *Gephyrocapsa* with open central area in unstable environments.

Although there is not a general agreement (e.g. Rontani et al., 2009, Rontani et al., 2013; Hoefs et al., 1998; Ausín et al., 2021; Rigual-Hernández et al., 2022), it is largely believed that the

relative proportions of the unsaturated alkenone compounds are preserved in the sediments because both $C_{37:2}$ and $C_{37:3}$ are eventually degraded equally (e.g. Prahl and Muehlhausen, 1989; Sikes et al., 1991; Teece et al., 1998; Grimalt et al., 2000). In support of this is the alkenone-based SST pattern, which does not deviate from what expected in tracing glacial/interglacial and stadial/interstadial phases, according to the $\delta^{18}O$ outline at Site 975 (Fig. 2), and in agreement with very similar alkenone-SST values and patterns recorded west of Iberian Margin (Rodrigues et al., 2017) and in the central Mediterranean (Marino et al., 2020) during the same time interval. Therefore, excluding selective alkenone compound degradation, coccolith dissolution and contribution of non-calcifying haptophyte to alkenone concentration in the Algero-Balearic basin as playing a major role, our data highlight the fact that distinct gephyrocapsid species/morphotypes have likely contributed to total C_{37} alkenone concentration by producing different amount of specific unsaturated alkenone compounds (Fig. 2G, blue and red lines; Fig. 3c–f) mainly in relation to SST changes (Fig. 3c and d). Surface water nutrient content and water mass circulation, in addition to temperature, influenced the gephyrocapsid proliferation during the peculiar oceanographic conditions that occurred through the warm ORL event in the early MIS 19c (Quivelli et al., 2020): shallow nutricline favored the higher percentage abundance (around 60%) of small *G. caribbeanica* (Fig. 2O violet line), a taxon with a seasonal blooming behavior (Baumann et al., 2005; Flores et al., 2012; Maiorano et al., 2013) that mostly contributed to total C_{37} alkenone concentration (401 ng/g at 784.7 ka) by producing the highest percentage of $C_{37:2}$ (Fig. 2N) and to higher total NAR (Fig. 2 D). The small *G. caribbeanica* seasonal bloom was likely promoted by the occurrence of obliquity and insolation maxima, which resulted in higher seasonal contrast during the early MIS 19c (Fig. 2). Although this issue is far from our aims, we can however sustain that orbital parameters may have influenced coccolithophore diversity and coccolith size variation (Beaufort et al., 2021).

In order to include other taxa of Noelaerhabdaceae potentially capable of producing alkenones, we also considered *Pseudoemiliania lacunosa* and *Gephyrocapsa omega* that, in our record, occurred following the late MIS 19c upwards, with abundances lower than <5% (Fig. 2Q and R). These taxa apparently did not contribute significantly to the alkenone production during their occurrence from ca. 756 to 776 ka. This seems supported by the low values of Pearson correlation coefficients between *P. lacunosa* and $C_{37:3}$ and $C_{37:2}$ ($r = -0.1$, $p < 0.5$, $n = 38$, and + 0.1, $p < 0.5$, $n = 38$, respectively), and between *G.*

omega and $C_{37:2}$ (r = + 0.3, $p < 0.05$, $n = 38$) and $C_{37:3}$, ($r = -0.3$, $p > 0.045$, $n = 38$). *G. omega* could have weakly taken part in the production of C_{37} alkenones, but *P. lacunosa*, although considered a possible alkenone precursor in the eastern Mediterranean during the Pliocene (Athanasiou et al., 2017), was not a significant producer during the Early-Middle Pleistocene when gephyrocapsids dominated (Fig. 2 D, red line). Our data suggest the prominent role of Noelaerhabdaceae *G. caribbeanica* and *G. margerelii-G. muellerae* as producers of alkenone-C_{37} during the mid-Pleistocene in the Algero-Balearic Sea. Similar evidences have been found in the contemporaneous record from central Mediterranean (Maiorano et al., 2021) and during the latest 300 kyrs from core U1475 in the Indian Ocean (Tangunan et al., 2021), which document that *G. oceanica* (*G. margerelii-G. muellerae* at Site 975) and *G. caribbeanica* were likely the main alkenone-producing taxa during the Pleistocene, together with the modern *Emiliania huxleyi* during the latest Quaternary (Tangunan et al., 2021).

7. Conclusions

The high-resolution quantitative data-set acquired at the ODP Site 975 on the coccolithophore paleoproductivity proxies, total C_{37} alkenone concentration and nannofossil accumulation rate (NAR), for the first time has been combined with abundances of species and morphotypes, unsaturated C_{37} compounds, alkenone-derived SST and $\delta^{18}O_{G.bulloides}$ through the mid-Pleistocene late MIS 20-MIS 19. Our results enrich the knowledge on past productivity and its relationships with alkenone-producing species and main environmental variables. The most important indications are as follow:

- -he patterns of two coccolithophore paleoproductivity proxies and their relationship would suggest that even low/high NAR of the alkenone-producing species may have produced high/low amount of C_{37} alkenones depending on paleoenvironmental and paleoecological factors;
- temperature primarily controlled the abundance changes and repeated shifts through time between the most abundant taxa within gephyrocapsids, which were the main C_{37} alkenone-producing species;
- *G. caribbeanica* mostly produced the di-unsaturated $C_{37:2}$ whereas *Gephyrocapsa* with open central area (mainly *G. margerelii-G. muellerae*) produced $C_{37:3}$ during warm and cool-cold periods, respectively, coherently with their ecological preference and glacial-

interglacial and stadial-interstadial sea water temperature changes; the larger morphotypes (> 3 μm) of *G. margerelii-G. muellerae* likely contributed to the occurrence of $C_{37:4}$ during the colder late MIS 20 terminal stadial and the stadial phases of MIS 19a;

- the alkenone-SST pattern, in accordance with $\delta^{18}O_{G.\ bulloides}$ profile, depicts distinct glacial-interglacial and stadial-interstadial oscillations;
- other potential alkenone-producing species such as *P. lacunosa* apparently did not play a role in C_{37} alkenone production during the studied interval that was dominated by gephyrocapsids;
- in addition to temperature, other environmental and ecological factors may have impacted on past paleoproductivity: climatically-induced oceanographic condition (slow to shutdown of WMDW and higher nutrient availability in the photic zone) influenced the C_{37} alkenone production and organic matter preservation at the sea bottom during the deglaciation and especially early MIS 19c ORL deposition, favoring higher coccolithophore productivity with a dominance of blooming small *G. caribbeanica*, and the highest total C_{37} concentration into sediments.

CRediT authorship contribution statement

Maria Marino: Writing – review & editing, Conceptualization. **Teresa Rodrigues:** Investigation, Formal analysis, Conceptualization. **Ornella Quivelli:** Investigation, Formal analysis, Data curation, Writing – original draft. **Angela Girone:** Investigation, Conceptualization. **Patrizia Maiorano:** Investigation, Conceptualization. **Franck Bassinot:** Investigation, Formal analysis, Data curation, Conceptualization.

Declaration of Competing Interest

The authors declare that they have no known competing financial interests or personal relationships that could have appeared to influence the work reported in this paper.

Acknowledgments

The authors thank the Ocean Drilling Program for providing the samples of ODP Site 975 and two anonymous reviewers for improving the first version of manuscript. This research was financially supported by Geoscience PhD scholarship, Bari University (Italy), and benefited of instrumental upgrades from “Potenziamento Strutturale PONa3_00369 dell'Università degli

Studi di Bari, Laboratorio per lo Sviluppo Integrato delle Scienze e delle Tecnologie dei Materiali Avanzati e per dispositivi innovativi (SISTEMA)". This research was supported by Fondi di Ateneo 2018 assigned to Patrizia Maiorano (Bari). Marine and terrestrial biomarkers have been processed at the Instituto Português do Mar e da Atmosfera (Portugal). This study received Portuguese national funds from FCT – Foundation for Science and Technology through projects UIDB/04326/2020, UIDP/04326/2020, LA/P/0101/2020, and WarmWorld (PTDC/CTA-GEO/29897/2017). Coccolithophore assemblage analyses have been performed at the Dipartimento di Scienze della Terra e Geoambientali, Bari University (Italy). Oxygen isotope analyses have been performed at the Laboratoire des Sciences du Climat et de l'Environnement (LSCE, France, contribution n. 7505).

Data will be available on PANGAEA.

References

Amore, F. O., Flores, J. A., Voelker, A. H. L., Lebreiro, S. M., Palumbo, E., Sierro, F. J., 2012. A Middle Pleistocene Northeast Atlantic coccolithophore record: Paleoclimatology and paleoproductivity aspects. Marine Micropaleontology 90, 44-59.

Athanasiou, M., Bouloubassi, I., Gogou, A., Klein, V., Dimiza, M. D., Parinos, C., Skampa, E., Triantaphyllou, M. V., 2017. Sea surface temperatures and environmental conditions during the "warm Pliocene" interval (~ 4.1–3.2 Ma) in the Eastern Mediterranean (Cyprus). Global and planetary change, 150, 46-57.

Ausín, B., Flores, J.A., Bárcena, M.A., Sierro, F.J., Francás, G., Gutierrez- Arnillas, E., Hernández-Almeida, I., Martrat, B., Grimalt, J.O., Cacho, I., 2015a. Coccolithophore productivity and surface water dynamics in the Alboran Sea during the last 25 kyr. Palaeogeogr. Palaeoclimatol. Palaeoecol. 418, 126-140.

Ausín, B., Hernández-Almeida, I., Flores, J.-A., Sierro, F.J., Grosjean, M., Francés, G., Alonso, B., 2015b. Development of coccolithophore-based transfer functions in the western Mediterranean sea: a sea surface salinity reconstruction for the last 15.5 kyr. Clim. Past 11, 1635-1651.

Ausín, B., Haghipour, N., Bruni, E., Eglinton, T., 2021. The influence of lateral transport on sedimentary alkenone paleoproxy signals. Biosciences Discussion, https://doi.org/10.5194/bg-2021-204.

Bard, E., Arnold, M., Maurice, P., Duprat, J., Moyes, J., Duplessy, J. C., 1987. Retreat velocity of the North Atlantic polar front during the last deglaciation determined by 14C accelerator mass spectrometry. Nature 328(6133), 791.

Bard E., Rostek F., Turon J.-L., Gendreau S., 2000. Hydrological impact of Heinrich events in the subtropical northeast Atlantic. Science 289, 1321-1324.

Bassinot, F., Labeyrie, L., Vincent, E., Quidelleur, X., Shackleton, N., Lancelot, Y., 1994. The astronomical theory of climate and the age of the Brunhes-Matuyama magnetic reversal. Earth and Planetary Science Letters 126 (1-3), 91-108, doi:10.1016/012-821X(94)90244-5.

Baumann, K.-H., Bockel, B., Frenz, M., 2004. Coccolith contribution to South Atlantic carbonate sedimentation. In: Thierstein, H.R., Young, J. (Eds.), Coccolithophores From Molecular Processes to Global Impact. Springer, Berlin, pp. 367–402.

Baumann, K.H., Andruleit, H., Böckel, B., Geisen, M., Kinkel, H., 2005. The significance of extant coccolithophores as indicators of ocean water masses, surface water temperature, and paleoproductivity: a review. Paläontol. Z. 79, 93-112.

Beaufort, L., Bolton, C., Sarr, A.C., Suchéras-Marx, B., Rosenthal, Y., et al., 2021. Cyclic evolution of phytoplankton forced by changes in tropical seasonality. Nature 601, 79-84 (2022). https://doi.org/10.1038/s41586-021-04195-7.

Beltran, C., de Rafélis, M., Minoletti, F., Renard, M., Sicre, M.A., Ezat, U., 2007. Coccolith δ18O and alkenone records in middle Pliocene orbitally controlled deposits: high frequencytemperature and salinity variations of sea surface water. Geochem. Geophys.Geosyst. 8. http://dx.doi.org/10.1029/2006GC001483.

Beltran, C., Flores, J.A., Sicre, M.A., Baudin, F., Renard, M., de Rafélis, M., 2011. Long chain alkenones in the early Pliocene Sicilian sediments (Trubi Formation-Punta di Maiata section): implications for the alkenone paleothermometry. Palaeogeogr. Palaeoclimatol. Palaeoecol. 308:253–263. http://dx.doi.org/10.1016/j.palaeo.2011.03.017.

Benzohra, M., Millot, C. 1995. Characteristics and circulation of the surface and intermediate water masses off Algeria. Deep Sea Research Part I: Oceanographic Research Papers 42(10), 1803-1830.

Bogus, K.A., Zonneveld, K.A.F., Fischer, D., Kasten, S., Bohrmann, G., Versteegh, G.J.M., 2012. The effect of meter-scale lateral oxygen gradients at the sediment–water interface on selected organic matter-based alteration, productivity and temperature proxies. Biogeosciences 9, 1553–1570.

Bollmann, J., 1997. Morphology and biogeography of Gephyrocapsa coccoliths in Holocene sediments. Marine Micropaleontology 29, 319-350.

Bollmann, J., Baumann, K.-H., Thierstein, H.R., 1998. Global dominance of Gephyrocapsa coccoliths in the late Pleistocene: selective dissolution, evolution, or global environmental change? Paleoceanography 13, 517-529.

Bollmann, J., Henderiks, J., Brabec., B., 2002. Global calibration of Gephyrocapsa coccolith abundance in Holocene sediments for paleotemperature assessment. Paleoceanography 17(3),1035.

Bolton, C. T., Wilson, P. A., Bailey, I., Friedrich, O., Beer, C. J., Becker, J., Baranwal, S., Schiebel, R., 2010. Millennial-scale climate variability in the subpolar North Atlantic Ocean during the late Pliocene. Paleoceanography, 25(4).

Bordiga, M., Cobianchi, M., Lupi, C., Pelosi, N., Venti, N. L., Ziveri, P., 2014. Coccolithophore carbonate during the last 450 ka in the NW Pacific Ocean (ODP site 1209B, Shatsky Rise). Journal of Quaternary Science, 29(1), 57-69.

Brassell, S. C., Eglinton, G., Marlowe, I. T., Pflaumann, U., Sarnthein, M., 1986. Molecular stratigraphy: A new tool for climatic assessment, Nature, 320, 129–133, doi:10.1038/320129a0.

Brassell, S. C., Dumitrescu, M., and the ODP Leg 198 Shipboard Scientific Party, 2004. Recognition of alkenones in a lower Aptian porcellanite from the west-central Pacific, Org. Geochem., 35, 181–188, doi:10.1016/j.orggeochem.2003.09.003.

Bryden, H. L., Stommel, H. M., 1982. Origin of the Mediterranean outflow. J. Mar. Res. 40, 55-71.

Cacho, I., Grimalt, J. O., Sierro, F. J., Shackleton, N., Canals, M., 2000. Evidence for enhanced Mediterranean thermohaline circulation during rapid climatic coolings. Earth and Planetary Science Letters 183(3-4), 417-429.

Canals, M., Puig, P., De Madron, X.D., Heussner, S., Palanques, A., Fabres, J., 2006. Flushing submarine canyons. Nature 444, 354–357.

Capotondi, L., Girone, A., Lirer, F., Bergami, C., Verducci, M., Vallefuoco, M., Afferri, A., Ferraro, L., Pelosi, N., De Lange, G.J., 2016. Central Mediterranean Mid-Pleistocene paleoclimatic variability and its connection with global climate. Palaeogeogr. Palaeoclimatol. Palaeoecol. 442, 72–83.

Comas, M.C., Zahn, R., Klaus, A., et al., 1996. Proceedings of the Ocean Drilling Program, Initial Reports, v. 161, College Station, Texas, Ocean Drilling Program.

Conte, M.H., Eglinton, G., Madureira, L.A.S., 1992. Long-chain alkenones and alkyl alkenoates as paleotemperature indicators: their production, flux and early sedimentary diagenesis in the Eastern North Atlantic. Org. Geochem. 19, 287-298.

Conte, M. H., Volkman, J. K., Eglinton, G., 1994. Lipid biomarkers of the Prymnesiophyceae. The Haptophyte Algae (eds J.C. Green and B.S.C. Leadbeater), pp. 351-377. Clarendon Press, Oxford.351-377.

Conte, M. H., Thompson, A., Eglinton, G., Green, J. C., 1995. Lipid biomarker diversity in the coccolithophorid Emiliania huxleyi (prymnesiophyceae) and the related species Gephyrocapsa oceanica 1. Journal of Phycology 31(2), 272-282.

Conte, M. H., A. Thompson, D. Lesley, R. P. Harris, 1998. Genetic and physiological influences on the alkenone/alkenoate versus growth temperature relationship in Emiliania huxleyi and Gephyrocapsa oceanica, Geochimica et Cosmochimica Acta, 62, 51-68.

Conte, M. H, Sicre, M., Rühlemann, C., Weber, J. C., Schulte, S., Schulz-Bull, D., Blanz, T., 2006. Global temperature calibration of the alkenone unsaturation index (UK' 37) in surface waters and comparison with surface sediments.Geochem. Geophys. Geosyst. 7, Q02005, doi:10.1029/2005GC001054.

Cramp, A., O'Sullivan, G., 1999. Neogene sapropels in the Mediterranean: a review. Mar. Geol. 153, 11–28.

Dittert, N., Baumann, K.-H., Bickert, R., Henrich, R., Huber, R., Kinkel, H., Meggers, H., 1999. Carbonate dissolution in the deep sea: Methods, quantification and paleoceanographic application. In: Fischer, G., Wefer, G. (Eds.), Use of Proxies in Paleoceanography: Examples from the South Atlantic. Springer Verlag, Berlin, Heidelberg, pp. 255-284.

D'Ortenzio, F., Ribera d'Alcalà, M., 2009. On the trophic regimes of the Mediterranean Sea: a satellite analysis. Biogeosciences 6 (2), 139-148.

Emanuele, D., Ferretti, P., Palumbo, E., and Amore, F.O., 2015. Sea-surface dynamics and palaeoenvironmental changes in the North Atlantic Ocean (IODP Site U1313) during Marine Isotope Stage 19 inferred from coccolithophore assemblages: Palaeogeography, Palaeoclimatology, Palaeoecology 430, 104-117.

Epstein, B.L., D'Hondt, S., Quinn, J.G., Zhang, J., Hargraves, P.E., 1998. An effect of dissolved nutrient concentrations on alkenone-based temperature estimates. Paleoceanography 13, 122-126.

Epstein, B. L., D'Hondt, S., Hargraves, P. E., 2001. The possible metabolic role of C37 alkenones in Emiliania huxleyi, Org. Geochem., 32, 867–875.

Farrimond P. G., Eglinton P. G., and Brassell S. C., 1986. Alkenones in cretaceous black shales, Blake-Bahama basin, western North Atlantic. In Advances in Organic Geochemistry 1985 (eds. D. Leytaheuser and J. Rullkotter). Pergamon, Oxford, vol. 10, pp. 897–903.

Flores, J.A., Sierro, F.J., 1997. Revised technique for calculation of calcareous nannofossili accumulation rates. Micropaleontology 43, 321-324.

Flores, J.A., Gersonde, R., Sierro, F.J., 1999. Pleistocene fluctuations in the Agulhas Current retroflection based on the calcareous plankton record. Marine Micropaleontology 37, 1-22.

Flores, J. A., Filippelli, G. M., Sierro, F. J., and Latimer, J. C., 2012. The “White Ocean” Hypothesis: A Late Pleistocene Southern Ocean Governed by Coccolithophores and Driven by Phosphorus, Front. Microbiol., 3, 233, https://doi.org/10.3389/fmicb.2012.00233.

Frigola, J., Moreno, A., Cacho, I., Canals, M., Sierro, F. J., Flores, J. A., Grimalt, J. O., 2008. Evidence of abrupt changes in Western Mediterranean Deep Water circulation during the last 50 kyr: A high-resolution marine record from the Balearic Sea, Quat. Int. 181, 88-104, doi:10.1016/j.quaint.2007.1006.1016.

Fujiwara, S., Tsuzuki, M., Kawashi, M., Minaka, N., Inouye, I., 2001. Molecular phylogeny of the haptophyta based on the rbcL gene and saquence variation in the spacer region of the RUBISCO operon. J Phycol 37,121681 129.

Giraudeau J., Grelaud M., Solignac S., Andrews J.T., Moros M., Jansen E. (2010) - Millennial-scale variability in Atlantic water advection to the Nordic Seas derived from Holocene coccolith concentration records. Quaternary Science Reviews 29, 1276-1287.

Girone, A., Capotondi, L., Ciaranfi, N., Di Leo, P., Lirer, F., Maiorano, P., Marino, M., Pelosi, N., Pulice, I., 2013. Paleoenvironmental change at the lower Pleistocene Montalbano Jonico section (southern Italy): global versus regional signals: Palaeogeography, Palaeoclimatology, Palaeoecology 371, 62-79.

Grimalt, J.O., Rullkötter, J., Sicre, M.-A., Summons, R., Farrington, J., Harvey, H.R., Goñi, M., Sawada, K., 2000. Modifications of the C37 alkenone and alkenoate composition in the water column and sediment: Possible implications for sea surface temperature estimates in paleoceanography, Geochemistry, Geophysics, Geosystems 691 1, n/a-n/a, 2000.

Harada, N., Shin, K.-H., Murata, A., Uchida, M., Nakatani, T., 2003. Characteristics of alkenones synthesized by a bloom of Emiliania huxleyi in the Bering Sea, Geochim. Cosmochim. Acta 67, 1507-1519. doi:10.1016/S0016694 7037(02)01318-2.

Harada, N., Sato, M., Shiraishi, A., Honda, M.C., 2006. Characteristics of alkenone distributions in suspended and sinking particles in the northwestern North Pacific. Geochim. Cosmochim. Acta 70, 2045–2062.

Henderiks, J., Pagani, M., 2007. Refining ancient carbon dioxide estimates: Significance of coccolithophore cell size for alkenone-based pCO2 records, Paleoceanogr., 22, PA3202, doi:10.1029/2006PA001399.

Henderiks, J., Pagani, M. 2008. Coccolithophore cell size and the Paleogene decline in atmospheric CO2. Earth 700 Planet. Sci. Lett. 269, 576–84.

Herbert, T. D., 2001. Review of alkenone calibrations (culture, water column, and sediments). Geochemistry, Geophysics, Geosystems, 2(2). Herbert, T. D., 2014. Alkenone Paleotemperature Determinations. In H. D. Holland, & K. K. Turekian (Eds.), Treatise on Geochemistry (2nd ed., Vol. 8, pp. 399–433). Elsevier. https://doi.org/10.1016/b978-0-08-095975705 7.00615-x.

Hoefs, M.J.L., Versteegh, G.J.M., Rijpstra, W.I.C., de Leeuw, J.W., Damsté, J.S.S., 1998. Postdepositional oxic degradation of alkenones: Implications for the measurement of palaeo sea surface temperatures. Paleoceanography 13, 42-49.

Jimenez-Espejo, F. J., Martinez-Ruiz, F., Rogerson, M., González-Donoso, J. M., Romero, O. E., Linares, D., Sakamoto, T., Gallego-Torres, D., Rueda Ruiz, J. L., Ortega-Huertas, M., Perez Claros, J. A., 2008. Detrital input, productivity fluctuations, and water mass circulation in the westernmost Mediterranean Sea since the Last Glacial Maximum. Geochemistry, Geophysics, Geosystems 9(11).

Jimenez-Espejo, F. J., Martinez-Ruiz, F., Sakamoto, T., Iijima, K., Gallego-Torres, D., Harada, N., 2007. Paleoenvironmental changes in the western Mediterranean since the last glacial maximum: high resolution multiproxy record from the Algero–Balearic basin. Palaeogeography, Palaeoclimatology, Palaeoecology 246(2716 4), 292-306.

Kitamura, E., Kotajima, T., Sawada, K., Suzuki, I., Shiraiwa, Y., 2018. Cold-induced metabolic conversion of haptophyte di- to tri-unsaturated C37 alkenones used as palaeothermometer molecules. Sci. Rep., 8 (2018), 2196, https://doi.org/10.1038/s41598-018-20741-2.

Kulhanek, D. K., 2009. Calcareous nannoplankton as paleoceanographic and biostratigraphic proxies: Examples from the mid-Cretaceous equatorial Atlantic (ODP leg 207) and Pleistocene of the Antarctic Peninsula (NBP0602A) and North Atlantic (IODP Exp. 306), PhD Dissertation, Florida State Univ., College of Arts and Sciences.

Kulhanek, D. K., Voelker, A. H., Grützner, J., 2008. Centennial-scale nannoplankton productivity changes in the mid-latitude North Atlantic during Marine Isotope Stages 11–12: Evidence from IODP site 1313, Abstract PP11B-1395 presented at Fall Meeting 2008, AGU 727

Lascaratos, A., Roether, W., Nittis, K., Klein, B., 1999. Recent changes in deep water formation and spreading in the eastern Mediterranean Sea: a review. Progress in oceanography, 44(1-3), 5-36. Leaman, K. D., Schott, F. A., 1991. Hydrographic structure of the convection regime in the Gulf of Lions: Winter 1987. Journal of Physical Oceanography 21(4), 575-598.

Madureira, L.A.S., Conte, M.H., Eglinton, G., 1995. Early diagenesis of lipid biomarker compounds in North Atlantic sediments. Paleoceanography 10, 627–642.

Maiorano, P., Tarantino, F., Marino, M., De Lange, G.J., 2013. Paleoenvironmental conditions at Core KC01B (Ionian Sea) through MIS 13-9: evidence from calcareous nannofossil assemblages. Quat. Int. 288, 97-111.

Maiorano, P., Marino, M., Balestra, B., Flores, J.A., Hodell, D.A., Rodrigues, T., 2015. Coccolithophore variability from the Shackleton Site (IODP Site U1385) through MIS 16–10. Glob. Planet. Change 133, 35-48.

Maiorano, P., Bertini, A., Capolongo, D., Eramo, G., Gallicchio, S., Girone, A., Pinto, D., Toti, F., Ventruti, G., Marino, M., 2016a. Climate signatures through the Marine Isotope Stage 19 in the

Montalbano Jonico section (Southern Italy): a land-sea perspective: Palaeogeography, Palaeoclimatology, Palaeoecology 461, 341-361.

Maiorano, P., Girone, A., Marino, M., Kucera, M., Pelosi, N., 2016b. Sea surface water variability during the Mid-Brunhes inferred from calcareous plankton in the western Mediterranean (ODP Site 975). Palaeogeography, Palaeoclimatology, Palaeoecology 459, 229-248.

Maiorano, P., Herbert, T. D., Marino, M., Bassinot, F., Bazzicalupo, P., Bertini, A., Girone, A., Nomade, S., Ciaranfi, N., 2021. Paleoproductivity modes in central Mediterranean during MIS 20-MIS 18: Calcareous plankton and alkenone variability. Paleoceanography and Paleoclimatology 36, e2021PA004259. https://doi,org/10.1029/2021PA004259.

Malinverno, E., Prahl, F.G., Popp, B.N., Ziveri, P., 2008. Alkenone abundance and its relationship to the coccolithophore assemblage in Gulf of California surface waters. Deep Sea Res. I 55, 1118–1130.

Marino, M., Maiorano, P., Tarantino, F., Voelker, A., Capotondi, L., Girone, A., Lirer, F., Flores, J.-A., Naafs, B.D.A., 2014. Coccolithophores as proxy of seawater changes at orbital- to-millennial scale during middle Pleistocene Marine Isotope Stages 14–9 in North Atlantic core MD01-2446. Paleoceanography 29. http://dx.doi.org/10.1002/2013PA002574.

Marino, M., Girone, A., Maiorano, P., Di Renzo, R., Piscitelli, A., Flores, J-A., 2018. Calcareous plankton and the mid-Brunhes climate variability in the Alboran Sea (ODP Site 977). Palaeogeography, Palaeoclimatology, Palaeoecology 508, 91-106.

Marino, M., Girone, A., Gallicchio, S., Herbert, T., Addante, M., Bazzicalupo, P., Quivelli, O., Bassinot, F., Bertini, A., Nomade, S., Ciaranfi, N., Maiorano, P., 2020. Climate variability during MIS 20-18 as recorded by alkenone-SST and calcareous plankton in the Ionian Basin (central Mediterranean). Palaeogeography, Palaeoclimatology, Palaeoecology, 560, 110027. https://doi.org/10.1016/j.palaeo.2020.110027.

Marlowe, I. T., Green, J. C., Neal, A. C., Brassel, S. C., Elington, G., Course, P. A., 1984. Long chain (n-C37 C39) alkenones in the Prymnesiophyceae: Distribution of alkenones and their taxonomic significance, Br. Phycol. J. 19, 203-216.

Marlowe, I.T., Brassell, S.C., Eglinton, G., and Green, J.C., 1990. Long-chain alkenones and alkyl alkenoates and the fossil coccolith record of marine sediments. Chem. Geol., 88:349–375.

Martin, J. M., Elbaz-Poulichet, F., Guieu, C., Loÿe-Pilot, M. D., Han, G., 1989. River versus atmospheric input of material to the Mediterranean Sea: an overview. Marine Chemistry, 28(1-3), 159-182.

Martrat, B., Grimalt, J.O., Lopez-Martinez, C., Cacho, I., Sierro, F.J., Flores, J.-A., Zahn, R., Canals, M., Curtis, J.H., Hodell, D.A., 2004. Abrupt temperature changes in the western Mediterranean over the past 250,000 years Science, 306 (2004), pp. 1762-1765.

Max, L., Lembke-Jene, L., Zou, J., Shi, X., Tiedemann, R., 2020. Evaluation of reconstructed sea surface temperatures based on U37k' from sediment surface samples of the North Pacific. Quat. Sci. Rev. 243, 106496.

McClymont, E.L., Rosell-Mele, A., Haug, G.H., Lloyd, J.M., 2008. Expansion of subarctic water masses in the North Atlantic and Pacific oceans and implications for mid-Pleistocene ice sheet growth. Paleoceanography 23, PA4214.

Millot, C., 1990. The gulf of Lions' hydrodynamics. Continental Shelf Research 10(9-11), 885-894.

Millot, C., 1999. Circulation in the western Mediterranean Sea. J. Mar. Syst. 20, 423–442.

Müller, P. J., Cepek, M., Ruhland, G., Schneider, R. R., 1997. Alkenone and coccolithophorid species changes in late Quaternary sediments from the Walvis Ridge: Implications for the alkenone paleotemperature method, Palaeogeogr. Palaeoclimatol. Palaeoecol., 135, 71–96, doi:10.1016/S0031-0182(97)00018-7.

Müller, P. J., Kirst, G., Ruhland, G., Von Storch, I., Rosell-Melé, A., 1998. Calibration of the alkenone paleotemperature index U37K' based on core-tops from the eastern South Atlantic and the global ocean (60° N 60° S). Geochimica et Cosmochimica Acta, 62(10), 1757-1772.

Nomade, S., Bassinot, F., Marino, M., Simon, Q., Dewilde, F., Maiorano, P., Esguder, G., Blamart, D., Girone, A., Scao, V., Pereira, A., Toti, F., Bertini, A., Combourieu-Nebout, N., Peral, M., Bourles, D., Petrosino, P., Gallicchio, S., Ciaranfi, N., 2019. High-resolution foraminifer stable isotope record of MIS 19 at Montalbano Jonico, southern Italy: a window into Mediterranean climatic variability during a low-eccentricity interglacial. Quat. Sci. Rev. 205, 106–125.

Okada, H., Wells, P., 1997. Late Quaternary nannofossil indicators of climate change in two deep-sea cores associated with the Leeuwin Current off Western Australia. Palaeogeogr. Palaeoclimatol. Palaeoecol. 131 (3–4), 413–432.

Pancost, R.D., Freeman, K.H., Patzkowsky, M.E., 1999. Organic-matter source variation and the expression of a late Middle Ordovician carbon isotope excursion Geology 27 (1999), 1015-1018.

Palumbo, E., Flores, J.A., Perugia, C., Petrillo, Z., Voelker, A.H.L., Amore, F.O., 2013. Millennial scale coccolithophore paleoproductivity and surface water changes between 445 and 360 ka (Marine Isotope Stages 12/11) in the Northeast Atlantic. Palaeogeogr. Palaeoclimatol. Palaeoecol. 383-384, 27-41.

Pierre, C., Belanger, P., Saliège, J.F., Urrutiaguer, M.J., Murat, A., 1999. Paleoceanography of the western Mediterranean during the Pleistocene: oxygen and carbon isotope records at Site 975. In: Zahn, R., Comas, M.C., Klaus, A. (Eds.), Proc. ODP, Sci. Results. 161. Ocean Drilling Program, College Station, TX, pp. 481488. https://doi.org/10.2973/odp.proc.sr.161.266.1999.

Pinardi, N., Masetti, E., 2000. Variability of the large scale general circulation of the Mediterranean sea from observations and modelling: a review. Palaeogeography, Palaeoclimatology, Palaeoecology 158 (2000) 153173.

Pinardi, N., Arneri, E., Crise, A., Ravaioli, M., Zavatarelli, M., 2006. The physical, sedimentary and ecological structure and variability of shelf areas in the Mediterranean sea. The sea 27 (14), 1243-1330.

Pinot, J.M., López-Jurado, J.L., Riera, M., 2002. The CANALES experiment (1996-1998). Interannual, seasonal, and mesoscale variability of the circulation in the Balearic Channels. Prog. Oceanogr. 55 (3–4), 335–370.

Plancq, J. (2015). Identification Des Producteurs d'alcénones dans le Register Sédimentaire du Cénozoïque: Implications Pour l'utilisation Des Proxys de Paléo-température (U37k') et de Paléo-pCO2 Ph.D. Thesis (Vol. 1). L'universite Claude Bernard Lyon.

Plancq, J., Grossi, V., Henderiks, J., Simon, L., Mattioli, E., 2012. Alkenone producers during late Oligocene early Miocene revisited. Paleoceanography, 27, PA1202. https://doi.org/10.1029/2011PA002164.

Plancq, J. Mattioli, E., Pittet, B., Simon, S., Grossi, V., 2014. Productivity and sea-surface temperature changes recorded during the late Eocene–early Oligocene at DSDP Site 511 (South Atlantic). Palaeogeography, Palaeoclimatology, Palaeoecology 407, 34-44.

Plancq, J., Mattioli, E., Henderiks, J., Grossi, V., 2013. Global shifts in Noelaerhabdaceae assemblages during the late Oligocene–early Miocene. Marine Micropaleontology, 103, 40-50.

Poynter, J., Eglinton, G., 1991. The biomarker concept—strengths and weaknesses. Fresenius' journal of analytical chemistry, 339(10), 725-731.

Prahl, F. G., Wakeham, S. G., 1987. Calibration of unsaturation patterns in long-chain ketone compositions for palaeotemperature assessment. Nature 330, 367-369. https://doi.org/10.1038/330367a0.

Prahl, F.G., Sparrow, M.A., Wolfe, G.V., 2003. Physiological impacts on alkenone paleothermometry. Paleoceanography 18.

Raja, M., Rosell-Melé, A., 2021. Appraisal of sedimentary alkenones for the quantitative reconstruction of phytoplankton biomass, P. Natl. Acad. Sci. USA, 118, e2014787118, https://doi.org/10.1073/pnas.2014787118.

Rigual-Hernández, A.S., Sierro, F.J., Flores, J.A., Trull, T.W., Rodrigues, T., Martrat, B., Sikes, E.L., Nodder, S.D., Eriksen, R.S., Davies, D., Bravo, N., Sánchez-Santosj, J.M., Abrantes, F., 2022. Influence of environmental variability and Emiliania huxleyi ecotypes on alkenone-derived temperature reconstructions in the subantarctic Southern Ocean. Science of The Total Environment 812, 152474.

Quivelli, O., Marino, M., Rodrigues, T., Girone, A., Maiorano, P., Abrantes, F., et al. (2020). Surface and deep water variability in the Western Mediterranean (ODP Site 975) during insolation cycle 74: High-resolution calcareous plankton and molecular biomarker signals. Palaeogeography, Palaeoclimatology, Palaeoecology, 542, 109583. https://doi.org/10.1016/j.palaeo.2019.109583.

Quivelli, O., Marino, M., Rodrigues, T., Girone, A., Maiorano, P., Bertini, A., Niccolini, G., Trotta, S., Bassinot, F., 2021. Multiproxy record of suborbital-scale climate changes in the Algero-Balearic Basin during late MIS 20- Termination IX. Quaternary Science Reviews 260 (2021) 106916. https://doi.org/10.1016/j.quascirev.2021.106916.

Riebesell, U., Zondervan, I., Rost, B., Tortell, P.D., Zeebe, R.E., Morel, F.M.M., 2000. Reduced calcification in marine plankton in response to increased atmospheric CO2. Nature 407, 634-637.

Rodrigues, T., Alonso-García, M., Hodell, D. A., Rufino, M., Naughton, F., Grimalt, J. O., Voelker, A.H.L., Abrantes, F., 2017. A 1-Ma record of sea surface temperature and extreme cooling events in the North Atlantic: A perspective from the Iberian Margin. Quaternary Science Reviews 172, 118-130.

Rodrigues, T., Grimalt, J. O., Abrantes, F., Flores, J. A., Lebreiro, S., 2009. Holocene interdependences of changes in sea surface temperature, productivity, and fluvial inputs in the Iberian continental shelf (Tagus mud patch), Geochemistry Geophysics Geosystems 10, Q07U06, doi:10.1029/2008GC002367.

Rodrigues, T., Grimalt, J. O., Abrantes, F., Naughton, F., Flores, J. A., 2010. The last glacial–interglacial transition (LGIT) in the western mid-latitudes of the North Atlantic: Abrupt sea surface temperature change and sea level implications. Quaternary Science Reviews, 29(15-16), 1853-1862.

Rodrigues, T., Voelker, A. H. L., Grimalt, J. O., Abrantes, F., Naughton, F., 2011. Iberian Margin sea surface temperature during MIS 15 to 9 (580–300 ka): Glacial suborbital variability versus interglacial stability, Paleoceanography 26(1), doi:10.1029/2010PA001927, 2011.

Rontani, J.-F., Beker, B., Volkman, J.K., 2004. Long-chain alkenones and related compounds in the benthic haptophyte Chrysotila lamellosa Anand HAP 17. Phytochemistry 65, 117-126.
Rosell-Melé, A., 1998. Interhemispheric appraisal of the value of alkenone indices as temperature and salinity proxies in high-latitude locations. Paleoceanography, 13(6), 694-703.

Saavedra-Pellitero, M., Flores, J.A., Baumann, K.-H., Sierro, F.J., 2010. Coccolith distribution patterns in surface sediments of equatorial and southeastern Pacific Ocean. Geobios 43, 131-149.

Samtleben, C., Bickert, T., 1990. Coccoliths in sediment traps from the Norwegian Sea. Marine Micropaleontology, 16(1-2), 39-64.

Schubert, C. J., Villanueva, J., Calvert, S. E., Cowie, G. L., von rad, U., Schulz, H., and Berber, U., 1998. Stable phytoplankton community in the Arabia Sea over the last 200,000 years. Nature 394, 563-566.

Schulte, S., Rostek, F., Bard, E., Rullkötter, J., and Marchal, O., 1999. Variations of oxygen-minimum and primary productivity recorded in sediments of the Arabian Sea. Earth and Planetary Science Letters 173, 205221.

Seki, O., Kawamura, K., Sakamoto, T., Ikehara, M., Nakatsuka, T., Wakatsuchi, M., 2005. Decreased surface salinity in the Sea Okhotsk during the last glacial period estimated from alkenones. Geophys Res Lett 32(8). https://doi.org/10.1029/2004GL02217.

Shackleton, N.J., Berger, A., Peltier, W.R., 1990. An alternative astronomical calibration of the lower Pleistocene timescale based on ODP Site 677. Earth Environ Sci Trans R Soc Edinb 81 (4), 251-261. Shipboard Scientific Party, 1996. Site 975. In Comas, M.C., Zahn, R., Klaus, A., et al. (eds), Proc. ODP, Init. Repts., 161: College Station, TX (Ocean Drilling Program), 113–177. doi:10.2973/odp.proc.ir.161.105.

Sicre, M.-A., Ternois, Y., Miquel, J.-C., Marty, J.-C., 1999. Alkenones in the northwestern Mediterranean Sea: interannual variability and vertical transfer. Geophys. Res. Lett. 26, 1735-1738.

Sicre, M. A., Ternois, Y., Paterne, M., Boireau, A., Beaufort, L., Martinez, P., Bertrand, P., 2000. Biomarker stratigraphic records over the last 150 kyears off the NW African coast at 25 N. Organic Geochemistry, 31(6), 577-588.

Sierro, F.J., Hodell, D.A., Curtis, J.H., Flores, J.A., Reguera, I., Colmenero-Hidalgo, E., Bárcena, M.A., Grimalt, J.O., Cacho, I., Frigola, J., Canals, M., 2005. Impact of iceberg melting on Mediterranean thermohaline circulation during Heinrich events. Paleoceanography 20, PA2019.

Sikes, E.L., Farrington, J.W., Keigwin, L.D., 1991. Use of the alkenone unsaturation ratio U37k to determine past sea surface temperatures: core-top SST calibrations and methodology considerations. Earth and Planetary Science Letters 104, 36-47.

Sikes, E.L., Volkman, J.K., Robertson, L.G., Pichon, J.-J., 1997. Alkenones and alkenes in surface waters and sediments of the Southern Ocean: implications for paleotemperature estimation in polar regions. Geochim. Cosmochim. Acta 61, 1495–1505.

Sikes, E.L., O'Leary, T., Nodder, S.D., Volkman, J.K., 2005. Alkenone temperature records and biomarker flux at the subtropical front on the Chatham rise, SW Pacific Ocean. Deep-Sea Res. I Oceanogr. Res. Pap. 52, 721-748.

Steinmetz, J.C., 1994. Sedimentation of coccolithophores. In: Winter, A., Siesser,W.G. (Eds.), Coccolithophores. Cambridge University Press, London, pp. 179-197.

Tangunan, D., Berke, M. A., Cartagena-Sierra, A., Flores, J.-A., Gruetzner, J., Jiménez-Espejo, F., et al., 2021. Strong glacial-interglacial variability in upper ocean hydrodynamics, biogeochemistry, and productivity in the southern Indian Ocean. Communication Earth & Environment, 2, 2–80. https://doi.org/10.1038/s43247-021 00148-0.

Teece, M.A., Getliff, J.M., Leftley, J.W., Parkes, R.J., Maxwell, J.R., 1998. Microbial degradation of the marine prymnesiophyte Emiliania huxleyi under oxic and anoxic conditions as a model for early diagenesis: long chain alkadienes, alkenones and alkyl alkenoates. Organic Geochemistry 29, 863-880.

Tiedemann, R., Sarnthein, M., Shackleton, N.J., 1994. Astronomic timescale for the pliocene atlantic d18O and dust flux records of Ocean Drilling Program site 659. Paleoceanography 9 (4), 619-638. Toti, F., Bertini, A., Girone, A., Marino, M., Maiorano, P., Bassinot, F., Combourieu Nebout, N., Nomade, S., Buccianti, A., 2020. Marine and terrestrial climate variability in the western Mediterranean Sea during marine isotope stages 20 and 19. Quat. Sci. Rev. 43 https://doi.org/10.1016/j.quascirev.2020.106486.

Trotta, S., Marino, M., Maiorano, P., Girone, A., 2019. 2019. Climate variability through MIS 20-MIS 19 in core KC01B, Ionian basin (central Mediterranean Sea). Alp. Mediterr. Quat 32 (2), 1-15. https://doi.org/10.26382/AMQ.2019.10.

Tzedakis, P.C., Channell, J.E.T., Hodell, D.A., Kleiven, H.F., Skinner, L.C., 2012. Determining the natural length of the current interglacial. Nat. Geosci. 5. https://doi.org/10.1038/NGEO1358.

Rickaby, R.E.M., Bard, E., Sonzogni, C., Rostek, F., Beaufort, L., Barker, S., Rees, G., Schrag, D.P., 2007. Coccolith chemistry reveals secular variations in the global ocean carbon cycle? Earth Planet. Sci. Lett. 253 (12), 83-95.

Versteegh, G. J., Riegman, R., de Leeuw, J. W., Jansen, J. F., 2001. U37K' values for Isochrysis galbana as a function of culture temperature, light intensity and nutrient concentrations. Organic Geochemistry, 32(6), 785-794.

Villanueva, J., Calvo, E., Pelejero, C., Grimalt, J. O., Boelaert, A., Labeyrie, L., 2001. A latitudinal productivity band in the central North Atlantic over the last 270 Kyr: An alkenone perspective, Paleoceanography 16, 1-10.

Villanueva, J., Grimalt, J. O., 1997. Gas Chromatographic Tuning of the UK37 Paleothermometer, Analytical Chemistry 69(16), 3329-3332.

Villanueva, J., Grimalt, J. O., Labeyrie, L. D., Cortijo, E., Vidal, L., Louis-Turon, J., 1998. Precessional forcing of productivity in the North Atlantic Ocean. Paleoceanography 13, 561-571.

Villanueva, J., Flores, J.A., Grimalt, J.O., 2002. A detailed comparison of the Uk'37 and coccolith records over the past 290 kyears: implications to the alkenone paleotemperature method. Org. Geochem. 33, 897–905.

Volkman, J.K., 2000. Ecological and environmental factors affecting alkenone distributions in seawater and sediments. Geochem. Geophys. Geosyst. 1 doi: 2000GC000061.

Volkman, J. K., Jeffrey, S. W., Rogers, G. I., Nichols, P. D., Garland, C. D., 1989. Fatty acid and lipid composition of 10 species of microalgae used in mariculture. Journal of Experimental Marine Biology and Ecology 128, 219-240.

Volkman, J. K., Barrerr, S. M., Blackburn, S. I., Sikes, E. L., 1995. Alkenones in Gephyrocapsa oceanica: Implications for studies of paleoclimate. Geochimica et Cosmochimica Acta,59(3), 513-520.

Volkman, J. K., Eglinton, G., CoRNER, E. D., Forsberg, T. E. V., 1980. Long-chain alkenes and alkenones in the marine coccolithophorid Emiliania huxleyi. Phytochemistry 19(12), 2619-2622.

Weaver, P.P.E., Pujol, C., 1988. History of the last deglaciation in the Alboran Sea (western Mediterranean) and adjacent North Atlantic as revealed by coccolith floras. Paleogeogr. Paleoclim. Paleoecol. 64, 35-42.

Weaver, P. P. E., Chapman, M. R., Eglinton, G., Zhao, M., Rutledge, D., Read, G., 1999. Combined coccolith, foraminiferal, and biomarker reconstruction of paleoceanographic conditions over the past 120 kyr in the northern North Atlantic (59°N, 23°W). Paleoceanography 14, 336-349. https://doi.org/10.1029/1999PA900009.

Westerhausen, L., Poynter, J., Eglinton, G., Erlenkeuser, H., Sarnthein, M., 1993. Marine and terrigenous origin of organic matter in modern sediments of the equatorial East Atlantic: the d13C and molecular record. Deep-Sea Res. I 40 (5), 1087-1121.

Yamamoto, M., Shiraiwa, Y., Inouye, I., 2000. Physiological responses of lipids in Emiliania huxleyi and Gephyrocapsa oceanica (Haptophyceae) to growth status and their implications for alkenone paleothermometry. Org. Geochem. 31, 799-811.